J Mol Model (2008) 14:367–374
DOI 10.1007/s00894-008-0278-z

ORIGINAL PAPER

Molecular modeling studies of poly lactic acid initiation mechanisms

Ashok Khanna · Yamini S. Sudha · Sandeep Pillai · Swagat S. Rath

Received: 6 November 2007 / Accepted: 24 January 2008 / Published online: 26 February 2008

Abstract The two possible routes to synthesize poly (lactic acid) are polycondensation of the lactic acid and ring opening polymerization (ROP) of the lactide. This work involves molecular modeling of the polymerization initiation mechanisms using different initiators a) H_2SO_4 for polycondensation b) aluminum isopropoxide for coordination-insertion ROP c)methyl triflate for cationic ROP, and d) potassium methoxide for anionic ROP. For molecular modeling of PLA, we have benchmarked our approach using Ryner's work on ROP of L-lactide using stannous (II) 2-ethylhexanoate ($Sn(Oct)_2$) and methanol as initiators. Our values of -15.2 kcal mol^{-1} and -14.1 kcal mol^{-1} for enthalpy changes in the two steps of activated complex formation match with Ryner's. Geometric and frequency optimizations have been done on Gaussian'03 using B3LYP density functional theory along with the basis sets LANL2DZ for metal atoms and 6–31G* and 6–31G** for non metal atoms. The *kinetic rate constant* for each mechanism has been calculated using the values of energy of activation, change in enthalpy, Gibbs free energy, entropy and the partition functions from the Gaussian'03 output. Our polycondensation rate constant value of 1.07×10^{-4} se^{-1} compares well with 1.51×10^{-4} se^{-1} as reported by Wang. However, ROP rate constants could not be validated due to lack of experimental data.

A. Khanna (✉) · Y. S. Sudha · S. S. Rath
Department of Chemical Engineering, IIT Kanpur,
Uttar Pradesh 208016, India
e-mail: akhanna@iitk.ac.in

S. Pillai
Larsen and Turbo Ltd.,
Mumbai, Maharashtra, India

Keywords Anionic/ cationic ring opening polymerization · Density functional theory · Poly-condensation · Poly(lactic acid)

Introduction

Recent advances in biodegradable polymers have been spurred by intense interest in biomedical applications [1, 2]. Biodegradable polymers break down in physiological environments by macromolecular chain scission into smaller fragments, and ultimately into simple stable end-products [3]. The degradation may be due to aerobic or anaerobic microorganisms, or biologically active processes (e.g., enzyme reactions) or passive hydrolytic cleavage [4, 5]. Biodegradable polyesters, such as poly(lactic acid) (PLA), poly(glycolic acid) (PGA), and poly(lactic-co-glycolic acid) (PLGA), have been extensively studied for a wide variety of pharmaceutical and biomedical applications due to their controllable biodegradability, excellent biocompatibility, and high safety [6]. The need for a variety of drug formulations for different drugs and delivery pathways resulted in development of various types of block copolymers (e.g., diblock, triblock, multiblock, and star-shaped block) consisting of the biodegradable PLA, PGA, Poly(ethylene glycol) (PEG) and PLGA. They have the advantage of not requiring surgical removal after they serve their intended purposes. PEG/PLGA hydrogels are particularly attractive systems for pharmaceutical applications because of their biodegradability and good safety profile [7]. These polymers can deliver drugs through dissolution, diffusion, or osmosis [8]. "Smart polymers" that display a physiochemical response in nonlinear fashion to external stimuli (*i.e.*, temperature, pH, solvent, magnetic field, electric field, ultrasound, *etc.*) have been widely explored as potential drug-delivery systems [9]. PLA is currently

used in a number of biomedical applications, such as sutures, stents, dialysis media and drug delivery devices, but it is also evaluated as a material for tissue engineering [10].

Poly (lactic acid) is an eco-friendly biodegradable polymer, it can be made from renewable sources and it being a thermoplastic, high strength, high modulus polymer, is replacing the conventional non-degradable packaging material [11]. Other than this it has found many biomedical applications like suture threads and controlled drug delivery [12]. The possible routes to synthesize PLA are either polycondensation of the lactic acid or ring opening polymerization of the lactide. Lactide is a dimer obtained from the depolymerization of low molecular weight PLA. The ring opening polymerization of L-lactide to produce PLLA can be basically through coordination-insertion, cationic and anionic mechanisms.

The most common route of step growth polymerization of L-Lactic acid is using protonic acids as initiators, which produces high crystalline polymers and also decreases dimerization which lead to the formation of lactide rings [13, 14]. It has been reported by Kricheldorf and Serra [15] that lactide can undergo coordination-insertion mechanism using metal octoates, carboxylates, oxides, and alkoxides. Stannous octoate is the most popular initiator for coordination-insertion mechanism [16–18]. Aluminum alkoxides have also been found by Dubios et al. [19] to initiate the lactide ring opening through coordination-insertion by an acyl oxygen bond cleavage. Cationic ring opening with methyl triflate as the initiator obeys the chemical rules of nucleophilic substitution as indicated by Kricheldorf and Dunsing [20]. In this mechanism initially formed positively charged lactide ring is opened by an S_N2 attack of the triflate anion accompanied by Walden-inversion. Jedlinski et al. [21] have reported that in anionic polymerization, initiated by potassium methoxide, the methoxide anion attacks the carbonyl carbon atom in the monomer molecule resulting in acyl-oxygen bond scission and formation of the methyl ester dead-end group and the alcoholate species.

Molecular modeling

Leach [22] and Clark [23] have presented molecular modeling techniques to predict structures, energies and other properties of molecules. Ab-initio calculations with rigorous, non-parameterized molecular orbital treatment derived from first principles are favored in situations where no experimental information is available. Each molecular orbital (one electron function) Ψ_i is expressed as a linear combination of n basis functions Φ_m. A basis set is essentially a finite number of atomic-like functions over which the molecular orbital is formed via linear combination of atomic orbitals (LCAO).

$$\psi_i = \sum_{m=1}^{n} c_{mi}\Phi_m \tag{1}$$

Most ab-initio calculations employ Gaussian type orbital (GTO) basis sets in which each atomic orbital is made up of a number of Gaussian probability functions. The most commonly used *polarization basis set* (i.e., one including *d*-orbitals) in the Gaussian03 program [24] is 6–31G* [25, 26]. This basis set uses *six* primitive Gaussians for the core orbitals, a *three/one* split for the *s*- and *p*-valence orbitals, and a single set of six *d*-functions (indicated by the *asterisk*). Six *d*-functions (equivalent to five *d*- and one *s*-orbital) are used for computational convenience, although Gaussian programs can also handle basis sets with five real *d-orbitals*. McLean and Chandler [27] and Krishnan et al. [28] present the further development of 6–31G** basis set, in which a set of *p-orbitals* has been added to each hydrogen in the 6–31G* basis set.

The density functional theory (DFT), B3LYP [29] is the most relevant for the transition metal structures. It uses an exchange functional that mixes the nonlocal Fock exchange with the gradient corrected form proposed by Becke [30] and adds the functional correlation proposed by Lee et al. [31] based on the previous work of Colle and Salvetti [32, 33]. This method includes a mixture of Hartree–Fock and DFT exchange in addition to DFT correlation terms. The B3LYP method has been used to calculate the potential energy surface for the intermediate structures in the mechanisms. Eguiburu et al. [34] studied the ROP mechanism of L-lactide initiated by aluminum trialkoxides using semiempirical methods in combination with DFT methods. DFT has also been successfully used to investigate the mechanisms of olefin polymerization with metallocenes and late transition metal complexes [35–37]. Ryner et al. [38] did a mechanistic study of the ring opening polymerization of 1,5-Dioxepan-2-one and L-lactide with stannous octoate using B3LYP.

This work involves the molecular modeling of the initiation mechanisms for polycondensation and ring opening polymerizations (coordination-insertion, cationic, and anionic). Change in enthalpy, Gibbs free energy, entropy along with energy of activation, and the kinetic rate constant have been determined for each mechanism.

Computational details

Geometries and the energies of all the structures were optimized using the hybrid density functional method B3LYP. This popular and computationally relatively cheap

method predicts reliable geometries and energetic [39–49]. During the first step, the geometries of all the structures were first optimized using LANL2DZ basis function for the metal atoms and 6–31G** for all the non-metal atoms. The LANL2DZ was used, as this basis set is specifically designed for metal atoms, where only the ultimate and the penultimate shell influence the bonding, the effects due to the rest of the core electrons are negligible. This basis set takes the core and the nucleus as one and neglects its effects and only considers the effect of the ultimate and the penultimate shells on the bonding [50, 51]. 6–31G** was used for non-metal atoms as it is a lower level basis set designed for the first two rows of elements.

During the second stage of calculations, the geometries of all the structures were first optimized and then a frequency optimization was done to find the thermodynamic properties using the same basis function of LANL2DZ for the metal atom but 6–311G** for all the non-metal atoms, which is a higher level basis set for non metal atoms. Using the split basis approach of LANL2DZ and 6–31G** first and then LANL2DZ and 6–311G** helps in predicting which are reasonably very good geometries and the frequency analysis give the properties which are in good agreement with the experimental results.

Determination of the kinetic rate constant

The rate constant k of a chemical reaction or a transport process may be expressed in terms of measurable properties, such as atomic or molecular dimensions, atomic masses, and inter-atomic or intermolecular forces and differences in thermodynamic properties between the initial and transition states—e.g., free energy, entropy, and enthalpy. According to transition state theory rate constant is given by:

$$k = \frac{k_B T}{\mathrm{h}} e^{-\Delta H/RT} e^{(1+\Delta S/R)} \tag{2}$$

where kB is the Boltzmann constant and h is the Planck constant. ΔS, the entropy of activation, is the standard molar change of entropy when the activated complex is formed from reactants and ΔH, the enthalpy of activation, is the corresponding standard molar change of enthalpy.

Now let us consider the general reaction, where the monomer A is being initiated by the initiator I to form the activated complex A.C., which results in formation of the transition state T.S. and hence the product P.

$$A + I \overset{K_{eq}}{\leftrightarrows} A.C. \xrightarrow{k_i} T.S. \rightarrow P$$

Rate of the reaction is given by:

$$\text{Rate} = \mathrm{k_i}[A.C.] \tag{3}$$

A and I being in equilibrium with the activated complex:

$$[A.C] = K_{eq}[A][I] \tag{4}$$

where Keq = Probability of reactants forming the activated complex which will form the transition state which ultimately gives the product *Keq* can be calculated from:

$$K_{eq} = \frac{Q_{AC}}{Q_A Q_I} \tag{5}$$

Q is the partition function defined by:

$$\mathrm{Q_A} = \mathrm{Q_{ATrans.}} \times \mathrm{Q_{ARot.}} \tag{6}$$

Combining Eqs. (3) and (4)

$$Rate = k_i K_{eq}[A][I] \tag{7}$$

k_i is determined from Eq. (2).

Benchmarking

We benchmarked the work of Ryner et al. [38], i.e., the mechanistic study of ring opening polymerization of L-lactide. Ryner et al. calculated the energy of activation to be 20.6 kcal mol^{-1}, which was very close to the experimental result of 17±0.4 kcal mol^{-1} [52]. We did the calculation again using the same density functional theory B3LYP and basis sets LANL2DZ (for metal atoms) and 6–311G** (for nonmetal atoms) for the formation steps of the active species from methanol and stannous octoate. Enthalpies of activation for the two steps were -15.2 and -14.1 kcal mol^{-1}. Our results matched exactly with those reported by Ryner et al.

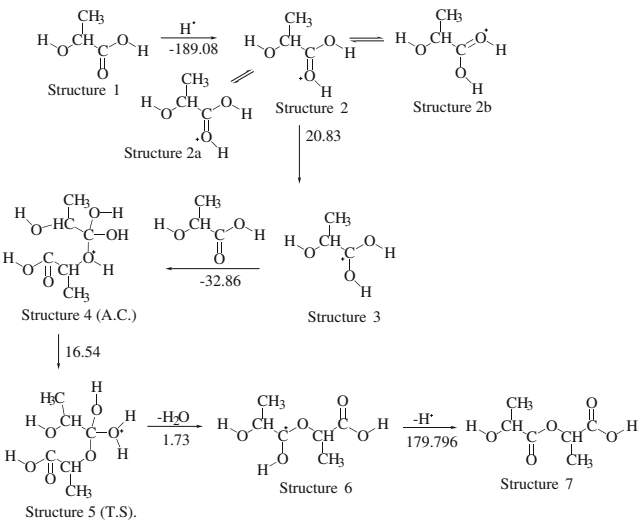

Fig. 1 Polycondensation mechanism of L-lactic acid. The numbers represent the change in energy in each step in kcal mol^{-1}

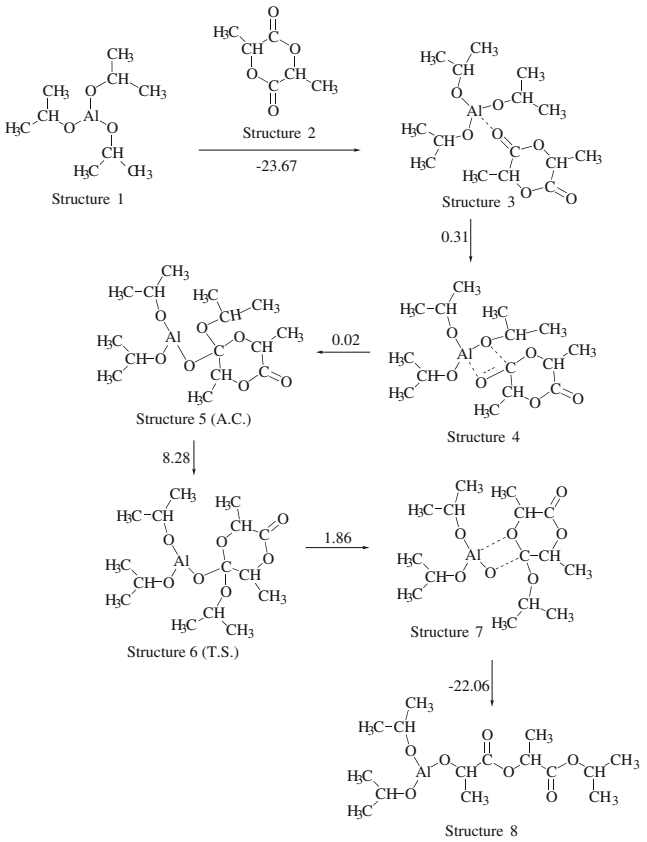

Fig. 2 Coordination insertion ring opening polymerization of L-lactide

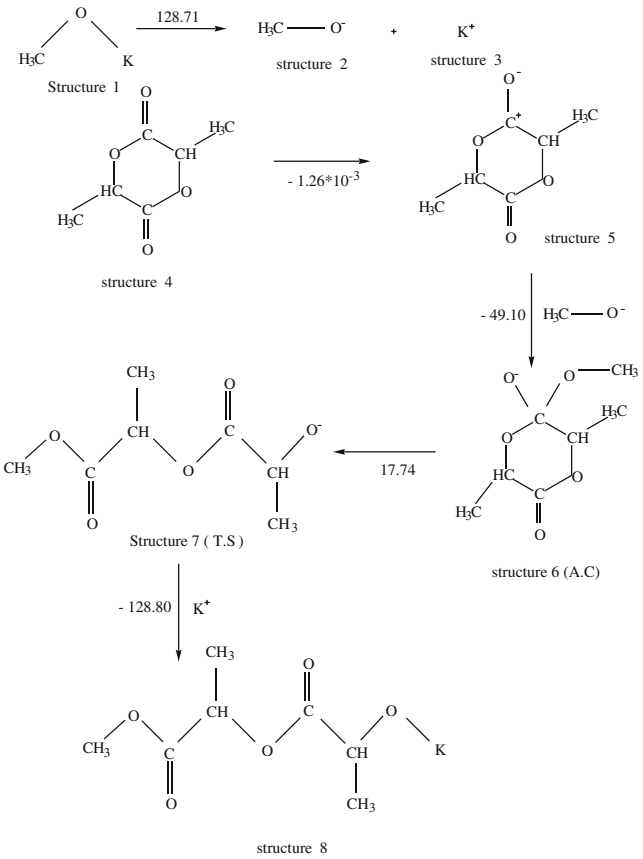

Fig. 4 Anionic ring opening polymerization of L-lactide

Results

The mechanism of PLA formation by poly-condensation has been illustrated in Fig. 1, where the numbers denote the energy difference (in kcal mol^{-1}) between two steps, as determined from the simulation. Figure 2 shows the mechanistic steps along with the energy changes for coordination insertion ring opening polymerization by aluminum isopropoxide. Similarly Fig. 3 and Fig. 4 shows the mechanistic steps involved in cationic ring opening polymerization by methyl triflate and anionic ring opening polymerization by potassium methoxide respectively.

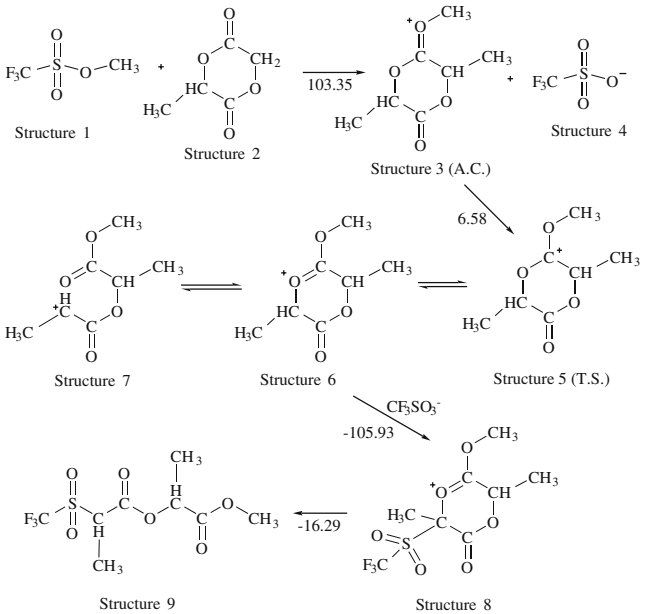

Fig. 3 Cationic ring opening polymerization of L-lactide

Tables 1 and 2 give the simulation results obtained from the Gaussian'03. The values obtained from Gaussian'03 are in Hartree/particle and they have been converted to kcal mol^{-1} by a conversion factor of 1 Hartree/Particle= 627.51 kcal mol^{-1}. Table 1 contains the changes in zero point energy (ΔZPE), energy (ΔE), enthalpy (ΔH), and Gibbs free energy (ΔG). Table 2 contains the entropies and partition functions of the structures relevant for the kinetics.

Determination of the kinetic rate expressions for the above mechanisms

Detailed calculation has been done to determine the kinetic rate expressions for the four mechanisms using Eqs. 2 to 7. Energy of activation ΔE and ΔH for the rate determining step have been determined from the Gaussian'03 simulation results given in Table 1. Relevant entropies and partition

Table 1 Changes in thermodynamic quantities during each step of polymerization

Energy diff in kcal mol^{-1}	Step I	Step II	Step III	Step IV	Step V	Step VI
a)Polycondensation	Str (2–1)	Str (3–2)	Str (4–3–1)	Str (5–4)	Str (6–2–5)	Str (7–6)
ΔZPE	-189.32	20.83	-26.88	10.88	1.84	179.69
ΔE	-189.08	20.83	-31.60	16.54	1.73	179.79
ΔH	-189.08	20.83	-32.31	16.54	2.43	179.79
ΔG	-189.49	20.79	-13.17	12.35	-9.42	177.84
b)Coord.Insertion ROP	Str (3–2+1)	Str (4–3)	Str (5–4)	Str (6–5)	Str (7–6)	Str (8–7)
ΔZPE	-22.47	0.36	0.018	8.75	1.58	-22.24
ΔE	-23.67	0.31	0.016	8.28	1.86	-22.06
ΔH	-24.37	0.31	0.016	8.026	1.86	-22.06
ΔG	-4.61	0.64	0.057	10.24	0.83	-24.24
c)Cationic ROP	Str (4+3- 2–1)	Str (5–4)	Str (6–5)	Str (7–6)	Str (8–6–3)	Str (9–8)
ΔZPE	102.92	6.57	0.00062	0.00062	-106.66	-16.98
ΔE	103.35	6.58	0	0	-128.79	-16.29
ΔH	103.35	6.58	0	0	-129.49	-16.29
ΔG	102.54	6.34	0.00025	0.00125	-71.87	-20.04
d)Anionic ROP	Str (2+3–1)	Str (5–4)	Str (6–5–2)	Str (7–6)	Str (8–7–3)	-
ΔZPE	129.09	-0.00125	-49.35	16.72	-128.96	-
ΔE	128.71	-0.00125	-49.10	17.74	-128.79	-
ΔH	129.41	-0.00125	-49.80	11.46	-129.49	-
ΔG	121.612693	- 0.002	-35.15	12.78	-118.86	-

functions have been listed in Table 2. The final results have been given in Table 3. Wang et al. [53] reported the rate expression as

$$-\frac{d[COOH]}{dt} = 1.51\times10^{-4}[COOH]^2$$

where as we have determined this to be Rate $= 1.070673\times 10^{-4}[LA]^2$.

Discussion

Polycondensation

L-lactic acid (Str. 1 in Fig. 1) reacts with another L-lactic acid molecule in presence of a concentrated protonic acid (mainly sulfuric acid) to produce poly (L-lactic acid). The reaction mixture is continuously distilled to remove water to prevent reversible reaction from happening [54]. The whole mechanism has been illustrated in Fig. 1.

In the first step of the reaction mechanism, the lactic acid molecule takes up a proton (a hydrogen ion), which is generated by the dissociation of sulfuric acid in the aqueous solution. The proton attaches itself to one of the lone pair of electrons of the oxygen (which is connected to the carbon atom with a double bond), of the carboxyl group in the lactic acid. The addition of the proton with the oxygen transfers the positive charge from the proton to the oxygen, thus creating a charged molecule. Oxygen being a highly electronegative atom always tries to attain stability by dispersing off any positive charge on it to other atoms connected to it. The case here is also the same; the positive charge given to the oxygen atom by the proton is dispersed on to the carbon atom attached to it. However, in the actual

Table 2 Entropy and partition functions of relevant structures for kinetics

Mechanism	Entropy (cal/mol K)			Partition functions		
	A.C	T.S		A	I	A.C
(a) polycondensation	130.037	130.626	Q_{trans}	0.512151D+08		0.124833D+09
			Q_{Rot}	0.183558D+06		0.127953D+07
(b) Coordination-insertion ROP	200.835	194.277	Q_{trans}	0.115D +09	0.104D+09	0.255D+09
			Q_{Rot}	0.30D+07	0.730D + 06	0.95D+07
(c) Cationic ROP	113.829	113.470	Q_{trans}	0.126D+09	0.104D+09	0.10895D+07
			Q_{Rot}	0.674D+06	0.730D+06	0.1203D+09
(d) Anionic ROP	117.800	131.830	Q_{trans}	0.351D+08	0.104D+09	0.139D+09
			Q_{Rot}	0.3055D+05	0.730D+06	0.127D+07

Table 3 Rate expressions for all four mechanisms

Mechanism	Rate determining step	Energy of activation (kcal mol^{-1})	ΔH for the rate determining step kcal mol^{-1}	ΔS for the rate determining step (Cal/mol K)	k_i (Sec^{-1})	$K_{eq} = \frac{Q_{A.C.}}{Q_A Q_I}$	Rate Expression $Rate = k_{ieq}[A][I]$
Polycondensation	IV	16.53	16.543	-3.411	2.526×10^{3}	4.237×10^{-8}	$1.07\times10^{-4}[LA]^2$
Coordination-insertion	IV	8.28	8.025	-6.558	7.92×10^{6}	1.31×10^{-9}	0.01042[A][I]
Cationic	II	6.58	6.58	-0.359	1.39×10^{9}	2.27×10^{-10}	0.318326 [A][I]
Anionic	IV	17.73	11.46	14.03	5.45×10^{7}	2.42×10^{-8}	1.324 [A][I]

case the positively charged ion is found to resonate between the three canonical structures (Structures 2, 2a and 2b). In the next step the positively charged carbon atom (Str.3) attracts another L-lactic acid molecule and makes a coordination bond with the lone pair of electrons from the oxygen atom in the alpha hydroxyl group. The formation of the coordination bond between the carbon atom and the oxygen atom transfers the positive charge from the carbon atom to the oxygen atom (Str.4). The step from structure 4 to structure 5 is the *rate controlling step* of the whole reaction (and can also be termed as a rearrangement step). The hydrogen attached to the positively charged oxygen, donates the electrons it had been sharing with the oxygen, to the positively charged oxygen and moves to bond with one of the hydroxyl oxygen attached to the carbon of the former carboxylic group. This transfer of hydrogen atom, from one oxygen to another also occurs with a transfer of charge from the first oxygen to the second. Now oxygen being a highly electronegative atom always tries to attain stability by dispersing off any positive charge on it to other atoms connected to it. In this case it transfers the positive charge back to the carbon atom of the former carboxylic group. This transfer of charge helps the oxygen atom to withdraw the electrons it had been sharing with carbon, for itself. This creates a water molecule. Now the presence of positive charge on the carbon atom (Str. 6) leads to an attraction of the electron clouds of the bonds joined to this carbon atom. This in turn creates a slight positive charge on the hydroxyl group oxygen attached to this carbon atom. This slight positive charge then pulls the electron cloud of the oxygen hydrogen bond toward itself. At the end of this tug of war, the hydrogen atom looses the bond pair electrons to the oxygen atom and is released as a proton. Now the bond pair of electrons from the oxygen hydrogen bond, transfers itself to the carbon. Thereby converting the carbon oxygen single bond to a double bond to form a carbonyl group (Str. 7).

Coordination insertion ring opening polymerization by aluminum isopropoxide

Initiation step of the reaction involves the carbonyl oxygen of the lactide ring (Str. 2 in Fig. 2) forming a weak hydrogen bond with the aluminum. This hydrogen bond has been found to be 1.97 Å long. The carbon of the carbonyl group of the lactide ring forms a bond with oxygen atom of one of the alkoxide groups (Str. 3). This bond formation leads to the formation of a four membered ring with aluminum and carbonyl oxygen on one side and carbonyl carbon and the alkoxide oxygen on one side (Str. 4). The carbon oxygen double bond in the carbonyl group looses its character and transforms itself into a bond which is not completely a single bond, which is evident from the bond length of 1.34 Å. Even the aluminum alkoxide bond changes from 1.73 Å to 1.96 Å. In the next step the transformation of the carbon oxygen double bond in the carbonyl group is complete and the alkoxide group attached to the aluminum breaks free from aluminum and forms a bond with the carbonyl carbon (Str. 5). Next comes the *rate controlling step* of the reaction. In this step the carbon alkoxide bond changes its position, thus transforming from structure 5 to structure 6, thus facilitating the acyl oxygen to come near the aluminum atom. This change in position is attained by the alkoxide group by revolving round the erstwhile carbonyl carbon atom. In the next step the acyl oxygen forms a bond with the aluminum atom and in this process stretches the acyl carbon oxygen bond (Str. 7). The bond length changes from 1.44 Å to 2.39 Å. This change eventually breaks the bond leading to the opening up of the ring. The aluminum oxygen (from the carbonyl group) also starts breaking in this step leading to the re-formation of the carbonyl group. The last step of the ring opening reaction of the lactide ring involves the completion of the acyl bond breakage. The formation of the carbonyl group is also complete. This gives us a new alkoxide group which is actually formed of the opened up lactide ring and the old alkoxide group (Str. 8).

Cationic ring opening polymerization by methyl triflate

The polymerization proceeds via triflate ester end group groups instead of free carbenium ions, which yield, at low temperatures of around 100°C, an optically active polymer without racemization. The propagation mechanism happens with the positively charged lactide ring being cleaved at the alkyl oxygen bond by an S_N2 attack of the triflate anion. The different steps in the cationic ring opening polymeri-

zation of L-lactide initiated by methyl triflate are detailed as follows (Fig. 3).

In the first step, the methyl triflate molecule (Str. 1) breaks down into negatively charged triflate ions (Str.4) and positively charged methyl ions. However, the positively charged methyl ions being highly unstable, they react with the nearby L-lactide ring (Str. 2) to form a positively charged methyl lactide ion (Str. 3), within an instant of their formation. The methyl carbocation's attack mainly happens on the carbonyl oxygen atom. This reaction gives the carbonyl oxygen a positive charge. This step is considered to be highly endothermic due to the breakage of methyl triflate molecule and the formation of the unstable methyl lactide ion. The second step of the reaction is just a transfer of charge from one atom to other, but this step is considered to be the *rate controlling step* of the reaction. In this step, the carbonyl oxygen, which by inherent nature is a highly electronegative atom, transfers the positive charge on to the carbonyl carbon. This transfer is attained by oxygen atom, as shown in structure 4, by taking up a bond pair of electrons from the carbonyl double bond and then converting it into a carbon oxygen single bond, as represented by structure 5. In the next step the charge on the carbon atom resonates through the ring, from the carbon (Str. 5) to the nearest acyl oxygen (Str. 6) and then to the next carbon atom (Str. 7) and back. The three structures act as resonating structures, where the electrons change position but not the atom. In this step the attack of the triflate ion on structure 6 happens. This attack leads to the formation of a complex (structure 8) which ultimately breaks down to form the product. The triflate ion attacks the carbon atom with the positive charge in structure 7. The complex, formed in the last step breaks down to form the product. The whole molecule changes its character from a ring backbone system to a straight chain system.

Anionic ring opening polymerization

As shown in Fig. 4, the reaction takes place with the dissociation of the potassium methoxide (Str. 1) initiator in the reaction mixture into negatively charged methoxide ions (Str. 2) and positively charged potassium ions (Str. 3). The actual initiator of the ring opening of L-lactide is the methoxide ion. The next step is not actually a reaction but is a rearrangement of partial charges in the monomer molecule. In this step the double bond in the carbonyl group of the monomer changes its character to a single bond. The main driving force of this change is the electro negativity of the oxygen atom of the carbonyl group. This drives a bond pair of electrons toward the oxygen atom, thus creating a negative charge on the oxygen atom and a positive charge on the carbon atom. It is this positive charge that helps in the nucleophilic attack in the latter steps of the reaction. Then the nucleophilic attack of the methoxide ion on the carbonyl atom takes place. This attack changes the very nature of the carbon oxygen double bond, this is evident from the fact that the bond length increases from 1.19 Å to 1.25 Å. The change is not restricted to the carbonyl group only, the acyl bond or the bond between the carbonyl carbon and oxygen on the ling backbone also changes its length from 1.44 Å to 1.58 Å thus helping the breakage of the acyl bond in the next step. In the next step from structure 6 to structure 7, the actual ring opening of the L-lactide occurs. This step is considered to be the *rate controlling step* of the whole reaction. In this step, the acyl bond which had increased its bond length to 1.58 Å in the last step breaks and opens up the L-lactide ring. This step creates a new propagating anion which attacks another monomer molecule and leads to its ring opening. In the termination step, the hydroxyl end group reacts with the positively charged potassium ions to give potassium salts of the polymer.

Conclusions

Kinetic rate expressions for the polymerization initiation mechanisms have been determined from the molecular modeling approach. Energy of activation, enthalpy change, Gibbs free energy change, and change in entropy have also been determined. Kinetic rate expression for the polycondensation mechanism is found to be in good agreement with the experimental result reported by Wang et al. [53]. Literature does not have rate expressions determined from experiments for the other mechanisms discussed here. Molecular modeling has been done for a single molecule initiated for the polymerization. So the rate constant, we determined corresponds to the initiation step of polymerization.

References

1. Eling B, Gogolewski S, Pennings AJ (1982) Polymer 23:1587–1593
2. Schmack G, Tandler B, Vogel R, Beyreuther R, Jacobsen S, Fritz H-G (1999) J Appl Polym Sci 73:2785–2797
3. Mooney DJ, Sano K, Kaufmann MP, Majahod K, Schloo B, Vacanti JP (1997) J Biomed Mater Res 37:413–420
4. Satyanarayana D, Chatterji PR (1993) Macromol Chem Phys C33:349–368
5. Griffith GL (2000) Polym Biomat Acta Mater 48:263–277
6. Gupta B, Revagade N, Hilborn J (2000) Prog Polym Sci 32:455–482
7. Singh S, Webster DC, Singh J (2007) Int J Pharm 341:68–77
8. Ikada Y, Tsuji H (2000) Macromol Rapid Commun 21:117–132
9. Chen S, Singh J (2005) Pharm Dev Technol 10:319–325
10. Lin PL, Fang HW, Tseng T, Lee WH (2007) Mater Lett 61:3009–3013
11. Stolt M, Sodergard A (2002) Prog in Polym Sci 27:1123–1163
12. Kulkarni RK, Pani KC, Neuman C, Leonard F (1966) Arch of Surg 93:839–843

13. Garlotta D (2001) J Polym Env 9(3):63–84
14. Mehta R, Kumar V, Bhunia H, Upadhyay SN (2005) J of Macro Sci 45:325–349
15. Kricheldorf HR, Serra A (1985) Polym Bull 14:497–502
16. Kricheldorf HR, Sumbel M (1989) Euro Poly J 25:585–591
17. Kohn FE, Van Den Berg JWA, Van de Ridder G, Feijen J (1984) J of App Poly Sci 29:4265–4277
18. Lille E, Rolf CS (1975) Makromoekulare Chemie 176(6):1901–1906
19. Dubios P, Jacobs C, Jerome R, Teyssie P (1991) Macromolecules 24:2266–2270
20. Kricheldorf HR, Dunsing R (1986) Makromoleculare Chemie 187:1611–1625
21. Jedlinski Z, Walach W, Kurcok P, Adamus G (1991) Makromoleculare Chemie 192:2051–2057
22. Leach AR (1996) Molecular Modelling: Principles and Applications. Pearson Education Limited
23. Clark T (1985) A Handbook of Computational Chemistry. John Wiley and Sons, New York
24. Frisch MJ, Trucks GW, Schlegel HB, Scuseria GE, Robb MA, Cheeseman JR, Montgomery JA, Vreven T, Kudin KN, Burant JC, Millam JM, Iyengar SS, Tomasi J, Barone V, Mennucci B, Cossi M, Scalmani G, Rega N, Petersson GA, Nakatsuji H, Hada M, Ehara M, Toyota K, Fukuda R, Hasegawa J, Ishida M, Nakajima T, Honda Y, Kitao O, Nakai H, Klene M, Li X, Knox JE, Hratchian HP, Cross JB, Adamo C, Jaramillo J, Gomperts R, Stratmann RE, Yazyev O, Austin AJ, Cammi R, Pomelli C, Ochterski JW, Ayala PY, Morokuma K, Voth GA, Salvador P, Dannenberg JJ, Zakrzewski VG, Dapprich S, Daniels AD, Strain MC, Farkas O, Malick DK, Rabuck AD, Raghavachari K, Foresman JB, Ortiz JV, Cui Q, Baboul AG, Clifford S, Cioslowski J, Stefanov BB, Liu G, Liashenko A, Piskorz P, Komaromi I, Martin RL, Fox DJ, Keith T, Al-Laham MA, Peng CY, Nanayakkara A, Challacombe M, Gill PMW, Johnson B, Chen W, Wong MW, Gonzalez C, Pople JA (2004) Gaussian 03, Revision C.02. Gaussian Inc, Wallingford
25. Dunning T (1970) J Chem Phys 53(7):2823–2833
26. Dunning Jr TH (1971) J Chem Phys 55(2):716–723
27. McLean AD, Chandler GS (1980) J Chem Phys 72(10):5639–5648
28. Krishnan R, Binkley RS, Seeger R, Pople JA (1980) J Chem Phys 72(1):650
29. Stevens PJ, Devlin FJ, Chablowski CF, Frisch MJ (1994) J Phys Chem 98(45):1623–11627
30. Becke AD (1998) Phys Rev A 38:3098
31. Lee C, Yang W, Parr RG (1980) Phys Rev B 37:785
32. Colle R, Salvetti O (1975) Theor Chim Acta 37:329
33. Colle R, Salvetti O (1979) Theor Chim Acta 53(1):55–63
34. Eguiburu JL, Fernandez-Berridi MJ, Cossio FP, SanRoman J (1999) Macromolecules 32(25):8252–8258
35. Yoshida T, Koga N, Morokuma K (1996) Organometallics 15 (2):766–767
36. Lohrenz JCW, Woo TK, Ziegler T (1995) J Am Chem Soc 117 (51):12793–12800
37. Musaev DG, Froese RDJ, Svensson M, Morokuma K (1997) J Am Chem Soc 119(2):367–374
38. Ryner M, Stritsberg K, Albertson A, Schenck HV, Svensson M (2001) Macromolecules 34(12):3877–3881
39. Musaev DG, Morokuma K (1996) J Phys Chem 100(16):6509–6517
40. Erikson LA, Pettersson LGM, Siegbahn PEM, Wahlgren U (1995) J Chem Phys 102(2):872–878
41. Ricca BCW (1994) J Phys Chem 98(49):2899–2903
42. Heinemann HRH, Wesendrup R, Koch W, Schwarz VH (1995) J Am Chem Soc 117(1):495–500
43. Hertwig RH, Hrusak J, Schroder D, Koch W, Schwarz H (1995) Chem Phys Lett 236(1,2):194–200
44. Schroder D, Hrusak J, Hertwig RH, Koch W, Schwerdtfeger P, Schwarz H (1995) Organometallics 14(1):312–316
45. Fiedler SD, Shaik S, Schwarz H (1994) J Am Chem Soc 116 (23):10734–10741
46. Fan L, Ziegler T (1991) J Chem Phys 95(10):7401–7408
47. Berces A, Ziegler T, Fan L (1994) J Phys Chem 98(6):1584–1595
48. Lyne PD, Mingos DMP, Ziegler T, Downs AJ (1993) Inorg Chem 32(22):4785–4796
49. Li J, Schreckenbach G, Ziegler T (1995) J Am Chem Soc 117 (1):486–494
50. Dunning TH (1970) J Chem Phys 53:2823
51. McLean AD, Chandler GS (1980) J Chem Phys 72:5639
52. Wiltzke DR, Narayan R, Kolstad JJ (1997) Macromolecules 30 (23):7075–7085
53. Wang Q, Zhang J (1994) Yingyong Huaxue 11(1):76–79
54. Hiltunen K, Seppala JV, Harkonen M (1997) Macromolecules 30:373–379